

# Synthesis of a New Series of Anthraquinone-Linked Cyclopentanone Derivatives: Investigating the Antioxidant, Antibacterial, Cytotoxic and Tyrosinase Inhibitory Activities of the Mushroom Tyrosinase Enzyme Using Molecular Docking

Janani Mullaivendhan<sup>1</sup>, Idhayadhulla Akbar<sup>1</sup>, Anis Ahamed<sup>2</sup>, Mansour K Gatasheh<sup>3</sup>, Ashraf Atef Hatamleh<sup>2</sup>, Gurusamy Raman<sup>4</sup>, Aseer Manilal<sup>5</sup>, Sabu Kuzhunellil Raghavanpillai<sup>6</sup>

<sup>1</sup>Research Department of Chemistry, Nehru Memorial College (Affiliated to Bharathidasan University), Puthanampatti, Tamil Nadu, 621007, India; <sup>2</sup>Department of Botany and Microbiology, College of Science, King Saud University, Riyadh, 11451, Saudi Arabia; <sup>3</sup>Department of Biochemistry, College of Science, King Saud University, Riyadh, 11451, Saudi Arabia; <sup>4</sup>Department of Life Science, Yeungnam University, Gyeongsan, Gyeongbuk-do, 38541, South Korea; <sup>5</sup>Department of Laboratory Sciences, College of Medicine and Health Sciences, Arba Minch University, Arba Minch, Ethiopia; <sup>6</sup>Biogeochemistry Division, VM Clays and Minerals, Thiruvananthapuram, Kerala, India

Correspondence: Aseer Manilal; Idhayadhulla Akbar, Email aseer.manila@amu.edu.et; a.idhayadhulla@gmail.com

**Purpose:** New bioactive anthraquinone derivatives are investigated for antibacterial, tyrosinase inhibitory, antioxidant cytotoxic activity, and molecular docking.

**Methods:** The compounds were produced using the grindstone method, yielding 69 to 89%. These compounds were analyzed using IR, <sup>1</sup>H, and <sup>13</sup>C NMR and elemental and mass spectral methods. Additionally, the antibacterial, antioxidant, and tyrosinase inhibitory activities of all the synthesised compounds were evaluated.

**Results:** Compound **2** showed remarkable tyrosinase inhibition activity, with an (IC<sub>50</sub>: 13.45 µg/mL), compared to kojic acid (IC<sub>50</sub>: 19.40 µg/mL). It also exhibited moderate antioxidant and antibacterial activities with respect to the references BHT and ampicillin, respectively. Kinetic analysis revealed that the tyrosinase inhibitory activity of compound **2** was non-competitive and competitive, whereas that of compound **1** was low. All compounds (1-8) were significantly less active than doxorubicin (LC<sub>50</sub>: 0.74±0.01µg/mL). However, compound **2** affinity for the **2Y9X** protein was lower than kojic acid, with a lower docking score (−8.6 kcal/mol compared to (−4.7 kcal/mol), making it more effective.

**Conclusion:** All synthesized compounds displayed remarkable antibacterial, tyrosinase inhibitory, antioxidant, and cytotoxic activities, with compound **2** showing exceptional potency as a multitarget agent. Anthraquinone substituent groups may offer the potential for the development of treatments. The derivatives were synthesized using the grindstone method, and their antibacterial, antioxidant, tyrosinase inhibitory, and cytotoxic activities were inspected. Molecular docking and molecular dynamics simulations were performed using compound **2** and kojic acid to validate the results and confirm the stability of the compounds.

**Keywords:** anthraquinone, tyrosinase enzyme, antioxidant activity, molecular docking, binding affinity, kojic acid, antibacterial activity, cytotoxic activity

## Introduction

Innovations in green chemistry can pave the way to environment-friendly processes and products with uncompromised bio-efficacy. Anthraquinone is an oxygen reduction reaction (ORR) catalyst due to its efficient redox capacity.<sup>1,2</sup> The synthesis of hydrogen peroxide for industrial use mainly depends on anthraquinone because it selectively reduces oxygen molecules to hydroperoxide radicals, and 10-hydroxy-9-anthracyl radicals are formed, which then undergo hydrogen abstraction, ultimately producing hydrogen peroxide and anthraquinone.<sup>1,3</sup> Fused heterocyclic systems can be found in various pharmaceutically

essential formulations and also in some natural products; many of them contain indeno furans, which are known to possess antibacterial and free radical scavenging properties. The indene derivatives are also well-known for their antibacterial properties.<sup>4</sup> Diethyl 4-cyano-2-hydroxy-5-oxo-4,5-dihydroindeno[1,2-b]pyran-3,4-dicarboxylate (13.2%) and diethyl-2,20-(1,3-dioxo-2,3-dihydro-1H-indene-2,2-diyl)bis(2-cyano acetate)<sub>2</sub> (15%) were two crystalline solid products.<sup>5,6</sup> Phytoalexins of plant origin are used in the treatment of various infectious diseases caused by different etiological agents.<sup>7</sup> Medical researchers have closely examined the diverse biological activities of many plant-derived molecules and marine natural products.<sup>8</sup> The controversy surrounding kojic acid stems from its toxicity.<sup>9</sup> Anthraquinone, a compound widely used in the cosmetic, medical, and agricultural industries, needs effective tyrosinase inhibitors with nominal side effects.<sup>10</sup>

Anthraquinone and its derivatives have been found to exhibit a variety of pharmacological effects, including anticancer,<sup>11</sup> anti-inflammatories,<sup>12</sup> antifungal,<sup>13</sup> antibacterial,<sup>14</sup> antiplatelet,<sup>15</sup> and neuroprotective properties.<sup>16</sup> Furthermore, these compounds exhibit desirable characteristics, such as significant emission, excitation, and absorption coefficients for visible wavelengths, as well as low toxicity.<sup>17,18</sup> Some of the natural products which are 2,3-dihydro-1 H inden-1-one are shown in Figure 1. Some of the natural products, 2,3-dihydro-1 H inden-1-one, are shown in Figure 1

Tyrosinase, an enzyme frequently present in nature, is reported to have a dinuclear copper core and possesses several functions (EC 1.14.18.1). It is often used to manufacture polyphenolic compounds and pigments like melanin.<sup>11</sup> The catalytic mechanism involving tyrosinase in the oxidation of phenols and diphenols depends on the active site, copper.<sup>19</sup> The copper present in this enzyme is responsible for its impressive catalytic activity in the first two steps, which involves the conversion of L-tyrosine into melanin. The process involves hydroxylating L-tyrosine to create L-dihydroxyphenylalanine (L-DOPA), which is further oxidized to form dopaquinone.<sup>20</sup>

Tyrosinase and similar proteins are synthesized in the rough endoplasmic reticulum. However, tyrosinase possesses some specificity related to malignant melanoma and enzymatic browning in mammals. Developing new and safer tyrosinase inhibitors is necessary for various applications across industries, such as food, cosmetics, dermatological products, and some medicines. Unfortunately, the number of inhibitors found suitable for clinical applications and skin whitening is limited; hence, there is a need for a continued search for natural and synthetic tyrosinase inhibitors. A recent review on tyrosinase inhibitors describes this aspect extensively.<sup>21</sup>

On the other hand, the pathophysiology of many diseases is significantly influenced by free radicals, and this is the reason for the growing interest in discovering and developing novel antioxidants that reduce the risk of damages caused by free radicals.<sup>22,23</sup> The use of antioxidants as preservatives in food items and dermatology, especially cosmetics, attracted more outstanding interests.<sup>24–26</sup> Due to their paramount importance as additives or antioxidants used to stop or slow down the natural occurrence of oxidation, they find diverse and extensive applications in producing numerous formulations.<sup>27</sup> Therefore, it is pivotal to discover novel tyrosinase inhibitors with enhanced efficacy and nil side effects.<sup>24</sup>

The purpose of conducting molecular docking studies is to understand better the results of in vitro activity studies, specifically regarding possible substrate preferences and variations in the active site of the target structure.<sup>28</sup> We have exploited the crystal structure of PPO3, a tyrosinase from *Agaricus bisporus* in its deoxy-form that includes an additional unidentified lectin-like subunit by means of anthraquinone-attached cyclopentanone derivatives. The inhibitor tropolone protein data bank (PDB ID code: **2Y9X**) was used for this purpose.<sup>29</sup> Using modern bioinformatics and cheminformatics tools, it is possible to create new anthraquinone-based chemical entities with a high degree of accuracy in terms of safety and efficacy. Additionally, the growing field of drug repurposing can be applied to discover new therapeutic uses for this scaffold, as given in some recent articles.<sup>11</sup>

Anthraquinone derivatives are well known for their antibacterial properties, especially against *E. coli* and *S. aureus*,<sup>30,31</sup> and also reported to act as antioxidants and exhibit tyrosinase activity.<sup>32,33</sup> Cosmetic products commonly use tyrosinase-inhibiting agents to preserve skin whiteness, and the use of antioxidants for skin lightening is based on the hypothesis involving oxidative processes.<sup>34</sup> The levels of phenolic and flavonoid compounds and their capacities for scavenging free radicals and inhibiting tyrosinase activity were closely related. The stronger the scavenging and inhibiting properties against free radicals and tyrosinase, the higher the concentration of antioxidants, such as kojic acid, which is known for its anti-tyrosinase and antioxidant properties.<sup>35</sup>

In a previous study, an interaction between tyrosinase and antioxidants was reported.<sup>36</sup> Therefore, the current study aimed to investigate anthraquinone-connected cyclopentanone derivatives as potential multitarget agents.

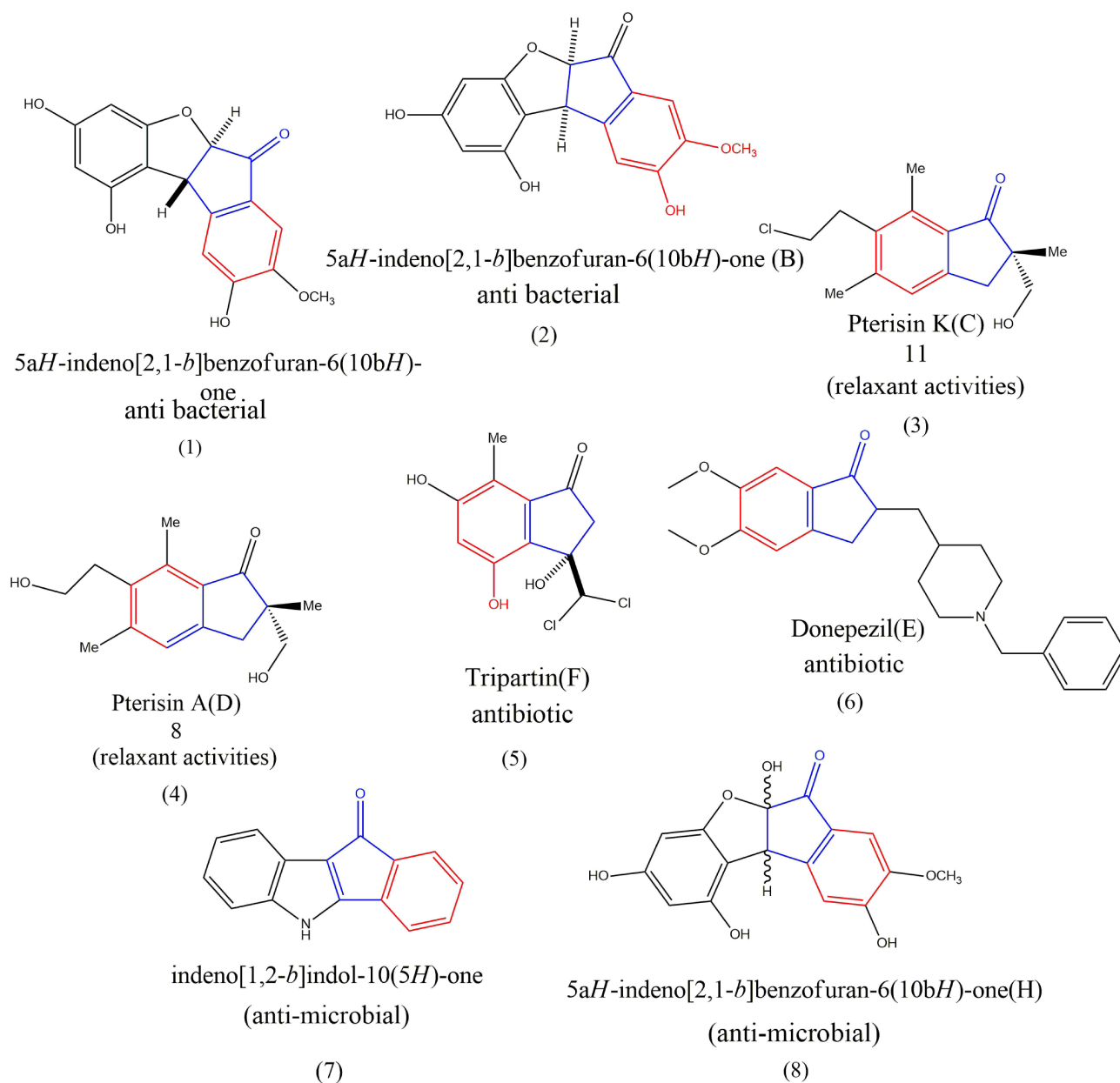


**Figure 1** Typical natural products based on 2,3-dihydro-1H inden-1-one.

Anthraquinone-connected cyclopentanone derivatives were synthesised using the grindstone method, and their antibacterial, antioxidant, tyrosinase inhibitory, and cytotoxic activities were inspected. Compound **2** was subjected to computational studies, including molecular docking and molecular dynamics simulations.

## Experimental Chemistry

A Thermo Scientific Nicolet iS5 FT-IR spectrometer (4000–400  $\text{cm}^{-1}$  range) and a Bruker DRX-300 MHz and 75 MHz instrument (for  $^1\text{H}$  and  $^{13}\text{C}$  NMR spectra analysis) were used to record the spectra of compounds. An elemental analyzer was used to determine the percentage of C, H, S, and N. Mass spectral analyses were performed by the hyphenated gas chromatography (GC-MS) Clarus SQ8 model from Perkin Elmer. All preparations were carried out using commercially available, general-purpose solvents and reagents, whereas analyses were performed using spectroscopic-grade solvents.

## Synthesis of compound 2,6,11-Trioxo-3-Phenyl-N-(o-Tolyl)-2,3,6,11-Tetrahydro-1H-Cyclopenta[a]anthracene-1-Carboxamide (I)

3-Oxo-N-(o-tolyl)butanamide (0.01 mmol), 1,4-dihydroxyanthracene-9,10-dione (0.01 mmol), and aromatic aldehydes (0.01 mmol) were mixed and ground for an hour at room temperature using the grindstone method. Thin layer chromatography (TLC) was used to determine the formation of new products after the reactions. The mixture was separated and purified by column chromatography using a solvent combination of ethyl acetate and hexane in a ratio of 4:6. All other compounds (2–8) were synthesised using the above method.

Yield 72%; mp 149°C; IR (cm<sup>-1</sup>): 2987 (Ar-NH), 3296 (NH), 1743 (C=O); <sup>1</sup>H NMR (300MHz, DMSO-d<sub>6</sub>): 8.29–7.88 (4H, Ar, d); 7.57–7.40 (d, Ar, 2H); 7.38–7.07 (4H, d, Ar); 7.23–6.77 (ph, m, 5H); 7.23 (1H, s, -NH); 4.92 (s, 2H, -CH<sub>2</sub>); 4.58 (s, CH<sub>2</sub>, 2H); 2.11 (s, -CH, 1H); <sup>13</sup>C NMR (75 MHz, DMSO-d<sub>6</sub>): 206.0 (1C, -C=O); 185.2–182.1 (2C, C=O); 147.2–128.9 (6C, Ar ring); 168.2 (1C, C=O); 147.2–128.9 (6C, Ar ring); 136.2–125.0 (6C, C=O); 133.6–126.8 (6C, Ar ring); 58.9 (1C, C=O); 58.4 (1C, -CH); 17.3 (1C, -CH<sub>3</sub>); EI-MS (*m/z*): 472.15 (M<sup>+</sup>, 33.9%); Elemental analysis: CalcdFor (C<sub>31</sub>H<sub>21</sub>NO<sub>4</sub>): C, 78.97; H, 4.49; N, 2.97% Found: C, 78.96; H, 4.52; N, 2.94%.

The spectral data of compounds (2–8) were reported in the [Figures S1-S16 Supporting Information](#).

## Biological Screening

### Tyrosinase Inhibitory Activity

A modified spectrophotometric method was employed to estimate the anti-tyrosinase activity using L-dopa as a substrate. All compounds (1–8) were dissolved in dimethyl sulfoxide (DMSO) to attain the required dilution. The mixture used in the reaction had a final volume of 3.0 mL and contained 1.5 mM L-DOPA, 0.1 mM sodium phosphate buffer with a pH of 6.5, and 12.42 U of mushroom tyrosinase. This mixture was preheated at 30°C and incubated for two minutes. The extent of dopachrome formation was determined by measuring the spectrophotometric absorbance at 475 nm using a Perkin Lambda 35 UV/VIS Spectrometer. Kojic acid was used as a positive control. The following expression gives the proportion of the inhibitory tyrosinase activity:

$$\text{Tyrosinase inhibitory activity (\%)} = (A - B) - (C - D) / (A - B) \times 100$$

The absorbance values of the control solution before and after incubation are denoted as A and B, respectively, whereas the absorbance values of the sample solution before and after incubation are denoted as C and D, respectively.<sup>37</sup>

### Antioxidant Activity

The addition of an antioxidant to a 1,1-diphenylpicrylhyrazyl (DPPH) solution in methanol at 517 nm causes the loss of the vibrant purple colour and a reduction in absorption. This indicates that the amount of residual 1,1-diphenylpicrylhyrazyl (DPPH) is inversely proportional to the level of antioxidant activity. The test compounds were added to 0.004% (w/v) methanolic solutions of 1,1-diphenylpicrylhyrazyl (DPPH) (4 mL) at various concentrations (25 or 100 µg/mL in methanol). The absorbance at 517 nm was measured after a 30-minute incubation period, and the percentage inhibition was calculated using the following formula.<sup>38</sup>

$$\text{Scavenging effect (\%)} = (A \text{ control} - A \text{ sample}) \times 100$$

Where, A sample: absorbance of the sample, A control: absorbance of DPPH solutions (except the test material, which contains all compounds); tests were carried out in triplicate.

### Antibacterial Activity

The antibacterial properties of the compounds were evaluated using the disc diffusion method, in which the compounds were dissolved in dimethyl sulfoxide (DMSO) at a concentration of 100 µg/mL. They were then impregnated into discs made of sterile filter paper (8 mm in diameter). Two type culture isolates were included, such as *S. aureus* (MTCC 96) and *E. coli* (MTCC 739). The bacterial test samples were prepared using sterile saline solution and pure colonies and the density was adjusted to reach a turbidity level of 0.5 McFarland standards. The test organisms were swabbed evenly over

Mueller-Hinton agar and exposed to a concentration gradient of compounds diffused from the impregnated paper disc into the agar medium. The inoculated and incubated plates were measured to find the zone of inhibition using ampicillin as a reference after a 24-hour incubation period at 37°C.<sup>32,39</sup>

## Minimum Inhibitory Concentration (MIC) Studies

The minimum inhibitory concentrations (MIC) of eight compounds were determined as shown in Table 3. The MIC, which signifies the lowest concentration of the microbial suspension that prevents visible growth of microorganisms, was determined by adding 10<sup>6</sup> CFU/mL to each well and then incubating the plates at 36°C for 24 h after preventing the visible growth of microorganisms.

## Cytotoxic Activity

In a previous study, the cytotoxicity of the newly developed compounds (1–8) was evaluated. The details of the experimental procedure are explained in a different context.<sup>39</sup>

## Statistical Analysis

All experiments were conducted in triplicate to ensure statistically validate the results. The data are represented as the mean standard deviation (S.D.) using the SPSS 25 version.

## Molecular Docking Analysis

Molecular docking experiments were performed using Schrödinger Maestro 9.2<sup>39</sup> to investigate the interactions and connections between the components of compound 1 and kojic acid, which is part of the most efficient anthraquinone series, with the proteins.

## Ligand Preparation

The compound structures (1–8) were designed using ChemDraw 12.0 and Chem3Dpro, which were subsequently employed in the creation of a Protein Data Bank (PDB) for docking studies.

## Receptor Preparation

The structure of the mosquito odourant-binding protein, which included water and ligands, was obtained from a protein database. To remove these, Discovery Studio 2019 was used, leaving only the receptors. To lower the energy of the receptor, the SWISS PDB Viewer was utilised, followed by a molecular docking process at the receptor.<sup>40</sup>

## Identification of the Binding Pocket

The co-crystallised ligand and Discovery Studio 2019 software were used to determine the presence of Asp 438, Asn 323, and Asn 332 residues within the pocket of the target protein.

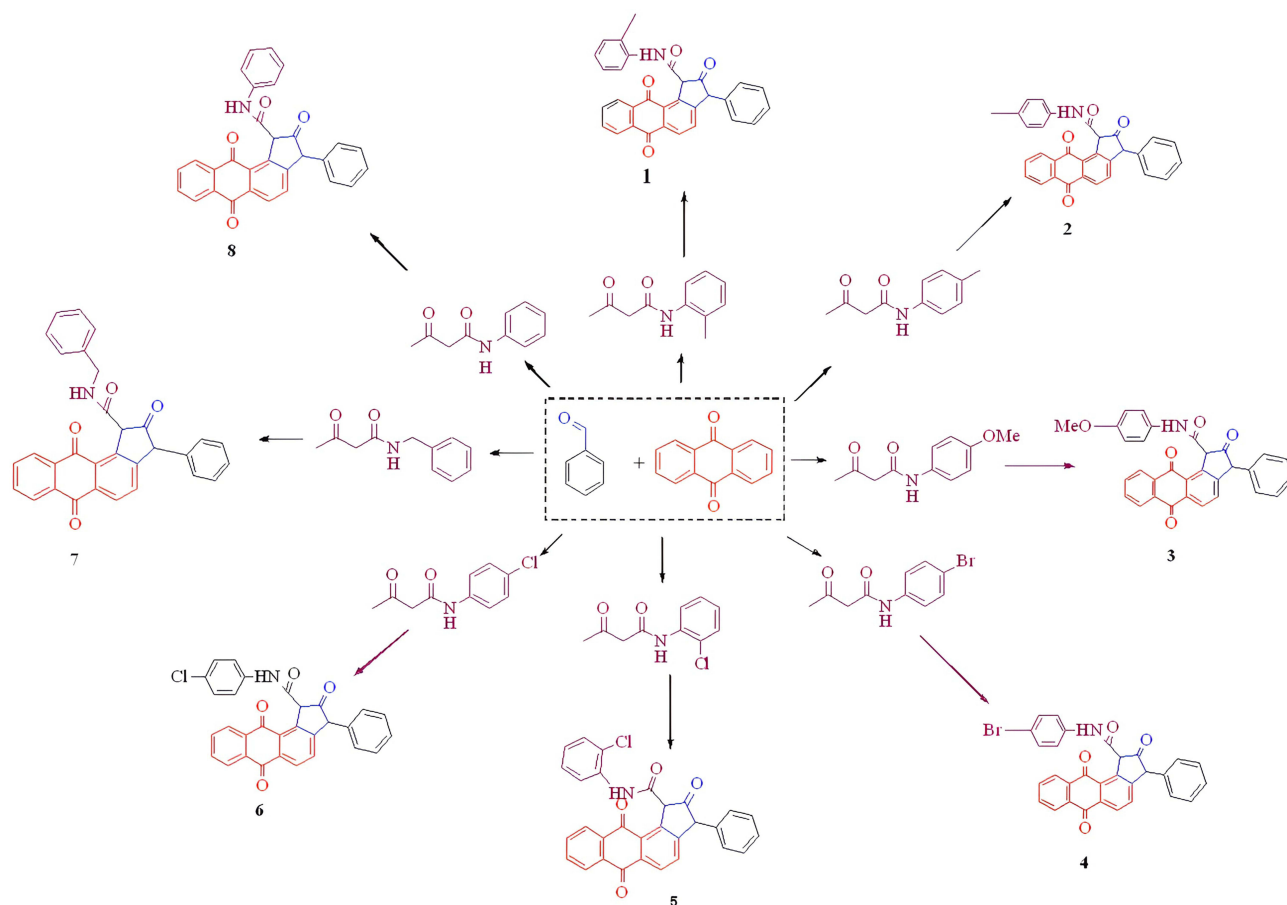
## Molecular Dynamics Simulation

Molecular dynamics simulations were performed using Desmond from Schrodinger Biosuite to assess the stability of the docked complexes identified through IFD analysis.<sup>41</sup>

## Results and Discussion

### Chemistry

By employing the Mannich base approach, multicomponent derivatives of anthraquinone were synthesized (one-pot synthesis). It was achieved through solvent-free green chemistry, as indicated in Scheme 1. FT-IR, <sup>1</sup>H, and <sup>13</sup>C NMR spectroscopies were employed to chemically analyse the target compounds. The IR spectra revealed significant bands at 2987–2665 cm<sup>-1</sup>, 3296–3168 cm<sup>-1</sup>, and 3296–3168 cm<sup>-1</sup>, which corresponded to the -Ar, -NH, and -CO groups, respectively. The aromatic rings, -Ar, -Ph, and -CH and -NH, were 8.29–6.80, 7.47–4.0, 4.77–4.58, and 7.17–4.64,



**Scheme 1** The synthesis of anthraquinone- cyclopentanone derivatives (**1–8**).

respectively, in the proton NMR spectra. In the  $^{13}\text{C}$  NMR spectra, peaks were observed at 206.0–54.5, 145.9–113.5, 140.3–21.9, 78.7–54.2, and 21.3–54.8 ppm; corresponding to the -Ph ring, -CH, -Ar ring, -CH<sub>3</sub>, -C=O, and -O-CH carbon, respectively. The results of elemental analysis and mass spectral patterns of each compound synthesized were perfectly consistent. All the data are available in the [Figures S1-S16 Supporting Information](#).

## Tyrosinase Inhibitory Activity

The tyrosinase inhibitory activity of various compounds was assessed using L-dihydroxyphenylalanine (L-DOPA) as a substrate, and the resulting percentage of inhibition is shown in [Figures 2–4](#). The test results of synthesized compounds were exactly opposite to those found for the inhibition of melanin formation.<sup>42,43</sup> The tyrosinase inhibitory activity of all synthesised compounds was evaluated using L-DOPA as the substrate by modifying a method previously reported by our research team, with slight modifications. This was done to evaluate their tyrosinase inhibitory activity.<sup>44</sup> Blocking the tyrosinase function requires a 4-hydroxyphenyl maollugin moiety with the correct species and placement of substituents in this series. Compound **2** showed an IC<sub>50</sub>: 13.45 µg/mL and was significantly more effective than kojic acid, having an IC<sub>50</sub>: 19.40 µg/mL, and these results are shown in [Table 1](#).

## Inhibitory Mechanism

The oxidation of l-dihydroxyphenylalanine (l-DOPA) by mushroom tyrosinase at various concentrations in relation to compounds **1** and **2** was examined (see [Figures S1-S16 Supporting Information](#) for complete details).

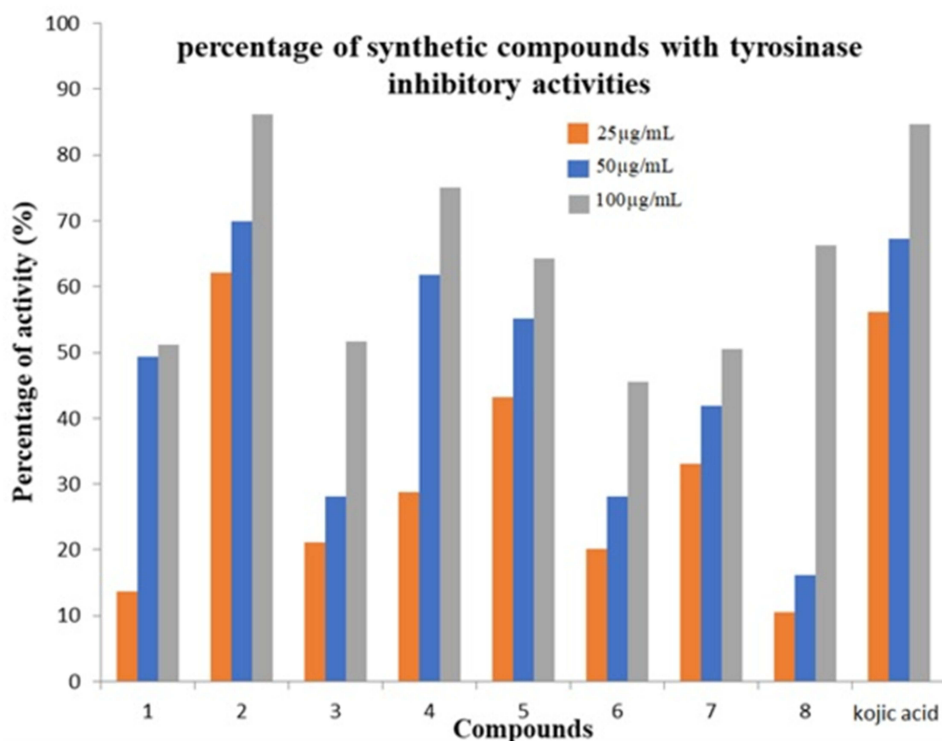


**Figure 2** Percentage of Tyrosinase Inhibitory activities of synthesized compounds (1–8) at concentration 100 µg/mL.

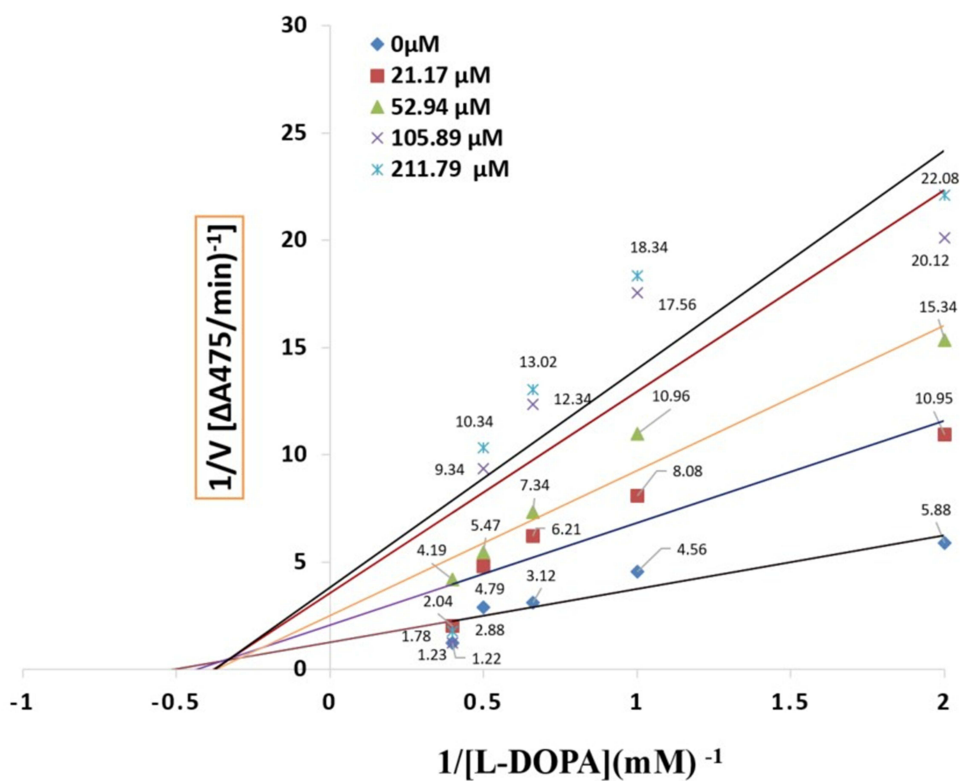


**Figure 3** Lineweaver-Burk plot for the inhibition of tyrosinase activity by compound I. Concentrations 0 µM, 21.17 µM, 52.94 µM, 105.89 µM and 211.79 µM were used for analysis compound I.

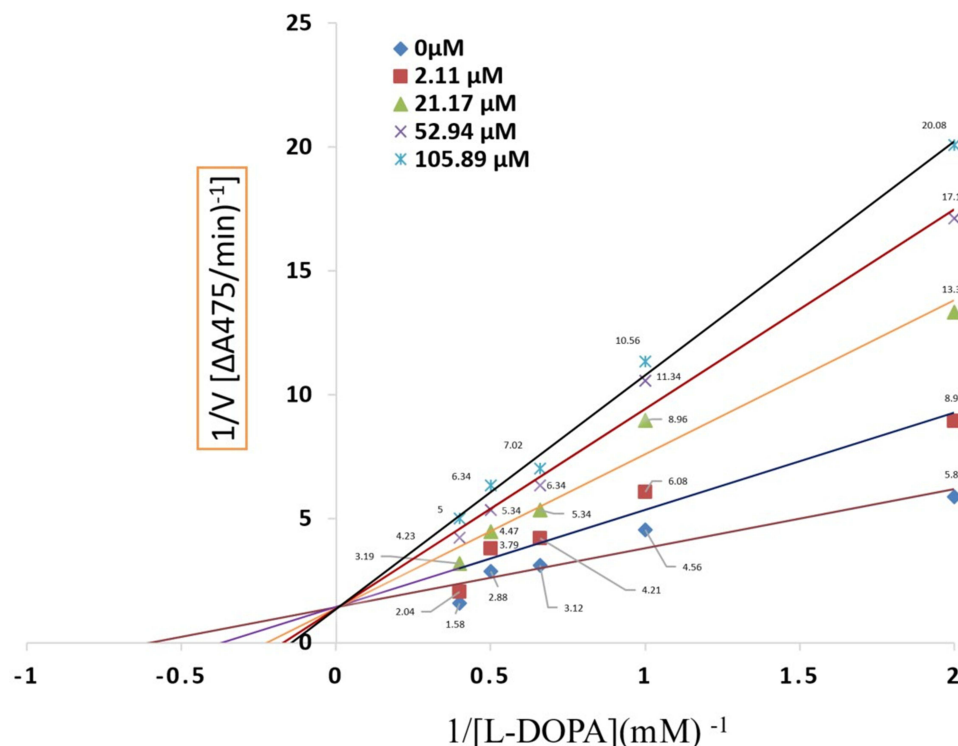


**Figure 4** Lineweaver Burk plot for the inhibition of tyrosinase activity by compound 2. Concentrations 0  $\mu\text{M}$ , 21.11  $\mu\text{M}$ , 21.17  $\mu\text{M}$ , 52.94  $\mu\text{M}$  and 105.89  $\mu\text{M}$  were used for analysis compound 2.

## Antioxidant Activity

Polyphenolic compounds are known to possess antioxidant properties. The radical-scavenging ability of the synthesised compounds was measured at 517 nm using a Perkin Lambda 35 UV/VIS Spectrometer, which detects phenolic hydroxyl groups. The 1,1-diphenylpicrylhydrazyl (DPPH) method was used to assess the free radical scavenging ability of the samples, with BHT serving as the reference compound and the samples were tested at concentrations of 25, 50, and 100  $\mu\text{g/mL}$ .<sup>32</sup> Additionally, the synthesised anthraquinone-cyclopentanone derivatives (1–8) were analysed for their ability to directly scavenge harmful nitrogen and oxygen-containing molecules, including 1,1-diphenylpicrylhydrazyl (DPPH). The results of the free radical scavenging activities are presented in Table 2, which displays the  $\text{IC}_{50}$  values and percentage inhibition for each synthetic substance. It was observed that all the synthesised compounds exhibited fair to excellent

**Table 1** Tyrosinase from Mushrooms Inhibitory Functions of Substances (1–8) and Standard Kojic Acid

Compound No.	Concentration ( $\mu\text{g/mL}$ ) <sup>a</sup>			$\text{IC}_{50}$ ( $\mu\text{g/mL}$ )
	25	50	100	
1	13.72 $\pm$ 0.02	49.30 $\pm$ 1.06	51.23 $\pm$ 0.23	77.62 $\pm$ 1.20
2	62.12 $\pm$ 0.12	70.00 $\pm$ 1.09	86.21 $\pm$ 1.52	13.45 $\pm$ 0.24
3	21.20 $\pm$ 0.23	28.11 $\pm$ 0.23	51.61 $\pm$ 1.06	87.31 $\pm$ 1.84
4	28.75 $\pm$ 0.21	61.87 $\pm$ 1.32	75.00 $\pm$ 1.36	42.65 $\pm$ 1.04
5	43.23 $\pm$ 0.15	55.21 $\pm$ 0.26	64.30 $\pm$ 1.52	63.22 $\pm$ 0.19
6	20.20 $\pm$ 0.11	28.12 $\pm$ 0.80	45.60 $\pm$ 0.26	>100
7	33.16 $\pm$ 1.0	41.95 $\pm$ 0.46	50.60 $\pm$ 1.08	99.98 $\pm$ 0.01
8	10.62 $\pm$ 0.52	16.25 $\pm$ 0.23	66.25 $\pm$ 0.81	80.16 $\pm$ 1.36
Kojic acid	56.23 $\pm$ 1.12	67.21 $\pm$ 1.12	84.65 $\pm$ 1.62	19.40 $\pm$ 0.74

**Note:** <sup>a</sup>The  $\text{IC}_{50}$  values represent means  $\pm$  SE of three different experiments.



**Table 2** Antioxidant Activity of Compounds (1–8)

Compound No.	Percentage of Activity (%)
	/mL
<b>1</b>	58.11
<b>2</b>	39.08
<b>3</b>	47.98
<b>4</b>	40.33
<b>5</b>	40.84
<b>6</b>	36.91
<b>7</b>	37.53
<b>8</b>	52.74
<b>BHT</b>	83.45

performance in 1,1-diphenylpicrylhydrazyl (DPPH) assays, demonstrating their potentials. The compound **6** has the lowest activity (36.91  $\mu\text{g/mL}$ ), while compound **1** has the highest (58.11  $\mu\text{g/mL}$ ), compared to standard BHT ( $\text{IC}_{50} = 83.45 \mu\text{g/mL}$ ) the results are shown in [Table 2](#).

## Antibacterial Studies

The antibacterial test results revealed that all compounds from (**1–8**) produced various degrees of inhibition ranging from 8 to 12 mm in diameter. The activity was relatively higher for the reference drug ampicillin, 23 and 17 mm. A negative control test using dimethyl sulfoxide (DMSO) demonstrated no inhibitory activity, proving that the solvent had no impact on bacterial growth ([Table 3](#)).<sup>45</sup>

**Table 3** Antibacterial Activities of Synthesized Compounds (1–8)

Compound No. ( $\mu\text{g/mL}$ )	Diameter of Growth Inhibition Zone (mm) <sup>a</sup> (Minimal Inhibitory Concentration (MIC, $\mu\text{g/mL}$ ) <sup>b</sup>	
	Gram-Positive Bacteria	Gram-Negative Bacteria
	<i>S. aureus</i>	<i>E. coli</i>
<b>1</b>	10(64)	– (>100)
<b>2</b>	10(64)	8 (>100)
<b>3</b>	8(>100)	– (>100)
<b>4</b>	8(>100)	– (>100)
<b>5</b>	12(64)	10(64)
<b>6</b>	12(64)	8(>100)
<b>7</b>	11(64)	8(>100)
<b>8</b>	11(64)	8(>100)
<b>Ampicillin</b>	23(0.5)	17 (1)
<b>DMSO</b>	–	–

**Note:** <sup>a</sup>Data are shown as mean  $\pm$  SD of three independent experiments.

**Abbreviation:** <sup>b</sup>MIC, minimal inhibitory concentration.

**Table 4** Cytotoxic Activities of Compounds (1–8)

Compounds	MCF-7			Normal Vero Cell Line	SI <sup>b</sup>
	GI <sub>50</sub> (μM)	TGI (μM)	LC <sub>50</sub> (μM)	LC <sub>50</sub> (μg/mL) <sup>a</sup>	
1	34.60 ± 0.65	60.1 ± 0.09	87.0 ± 0.16	93.01 ± 0.05	1.06
2	45.90 ± 0.43	67.4 ± 0.06	82.34 ± 0.16	91.03 ± 0.05	1.10
3	22.96 ± 0.03	45.28 ± 0.12	63.06 ± 0.02	68.12 ± 0.03	1.08
4	35.80 ± 0.07	45.34 ± 0.09	55.34 ± 0.05	80.30 ± 0.01	1.45
5	18.50 ± 0.04	24.6 ± 0.04	52.67 ± 0.02	78.33 ± 0.02	1.48
6	45.20 ± 0.03	67.23 ± 0.19	>100	87.16 ± 0.05	0.86
7	10.3 ± 0.12	18.04 ± 0.16	26.05 ± 0.85	65.60 ± 0.03	2.51
8	11.62 ± 0.19	22.01 ± 0.08	46.40 ± 0.05	54.96 ± 0.08	1.18
Doxorubicin	0.02 ± 0.00	0.21 ± 0.01	0.74 ± 0.01	19.85 ± 0.02	26.82

Notes: <sup>a</sup>Each value represents the mean ± standard deviation of three experiments. IC<sub>50</sub> value normal cell / IC<sub>50</sub> value cancer cell.

Abbreviation: <sup>b</sup>SI, Selectivity Index.

## Cytotoxic Activity

The synthesised compounds (1–8) were assessed for their cytotoxic effects against both MCF-7 and Vero cell lines, with all of them demonstrating low activity when compared to the standard drug doxorubicin (LC<sub>50</sub>:0.74 ± 0.01 μg/mL) as indicated in Table 4 (see Figures S1-S16 Supporting Information for comprehensive details). The Vero cell line was selected based on previous studies.<sup>44,46</sup>

## Docking

Molecular docking was conducted on compound 2 and kojic acid with 2Y9X, a protein that binds mosquito odourants.<sup>47</sup> Schrodinger Maestro 9.2 was used to study the interactions (Figures 5 and 6). The Pymol and

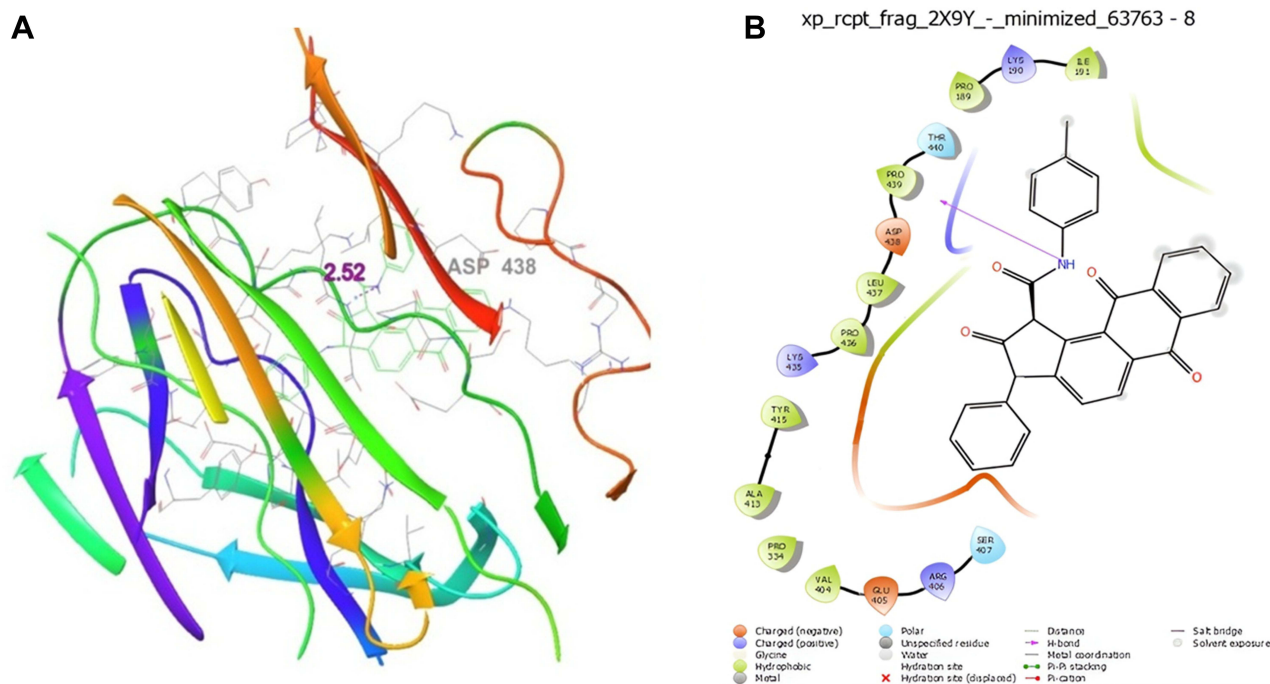


**Figure 5** Molecular docking studies on (A) compound 1 (3D Structure), (B) compound 1 (2D Structure) compound 1 docked with 2Y9X protein.

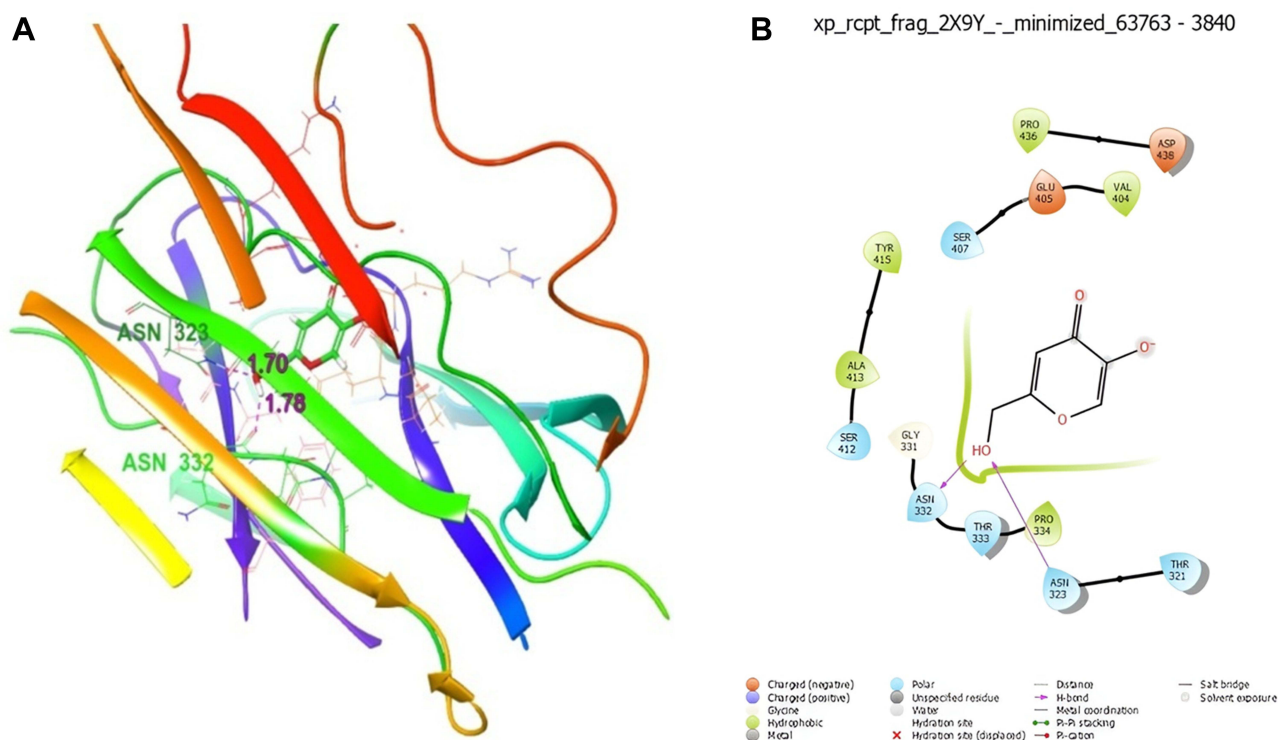


**Figure 6** Molecular docking studies on (A) Kojic acid (3D Structure), (B) Kojic acid (2D Structure) standard Kojic acid docked with 2Y9X protein.

Discovery Studio tools, which received a score of 8 for thoroughness, were used to evaluate the interactions. Two-dimensional molecular depictions were docked with compound 2 and kojic acid. The docking scores are listed in Table 5. (See [Figures S1-S16 Supporting Information](#) for full details)

## Molecular Dynamics Simulation

Molecular dynamics simulations were performed by Desmond and Schrödinger to dock the complex structures of ligand compound 2 with 2Y9X proteins.<sup>48</sup> In previous studies, we compared the molecular dynamics simulations to examine the interactions and stability of compounds with native ligands and kojic acid.<sup>49</sup> The stability and simulation of the complexes were analysed and are depicted in [Figures 7–10](#) (See [Figures S1-S16 Supporting Information](#) for full details).

## Structure-Activity Relationships

SAR studies of the anthraquinone ring structure offer valuable information into the essential structural features with predominant biological effects.<sup>50</sup> SAR studies have enabled the identification of groups that enhance the pharmacokinetics of the synthesised molecules and substituents that are resistant to enzymatic degradation. Some of the observations related to structure-activity relationships are discussed below [Table 6](#). (See [Figures S1-S16 Supporting Information](#) for full details)

**Table 5** Docked Result of Compound 2 and Drug with 2Y9X Using XP Method

S. No	Compound/Drug	Dock Score	Interacting Residues	Bond Length
1.	2	-8.6	Asp 438	2.52
2.	Kojic acid	-4.7	Asn 323, Asn 332	1.70, 1.78

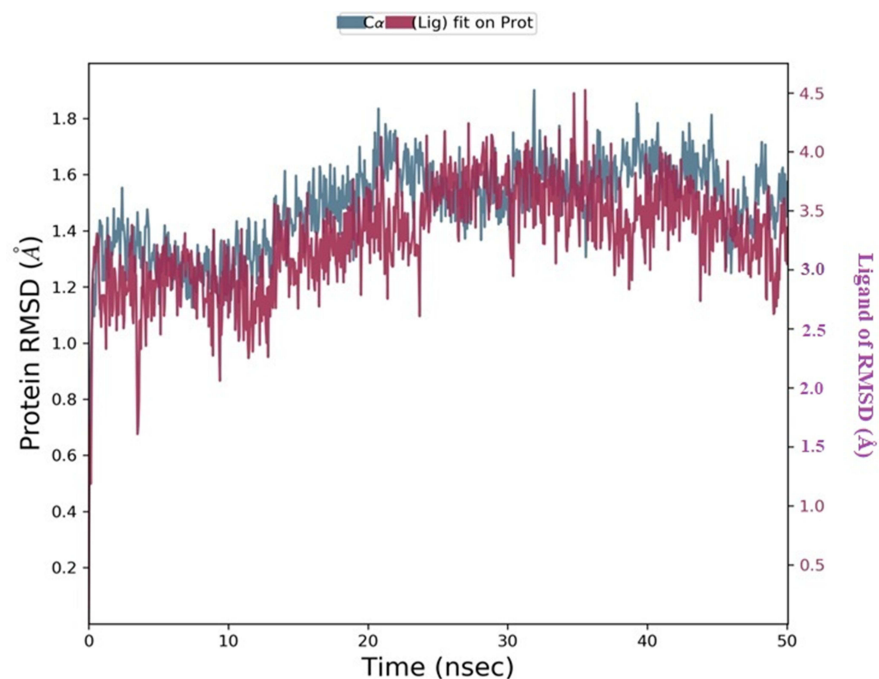


Figure 7 RMSD plot of 2Y9X with compound 2.

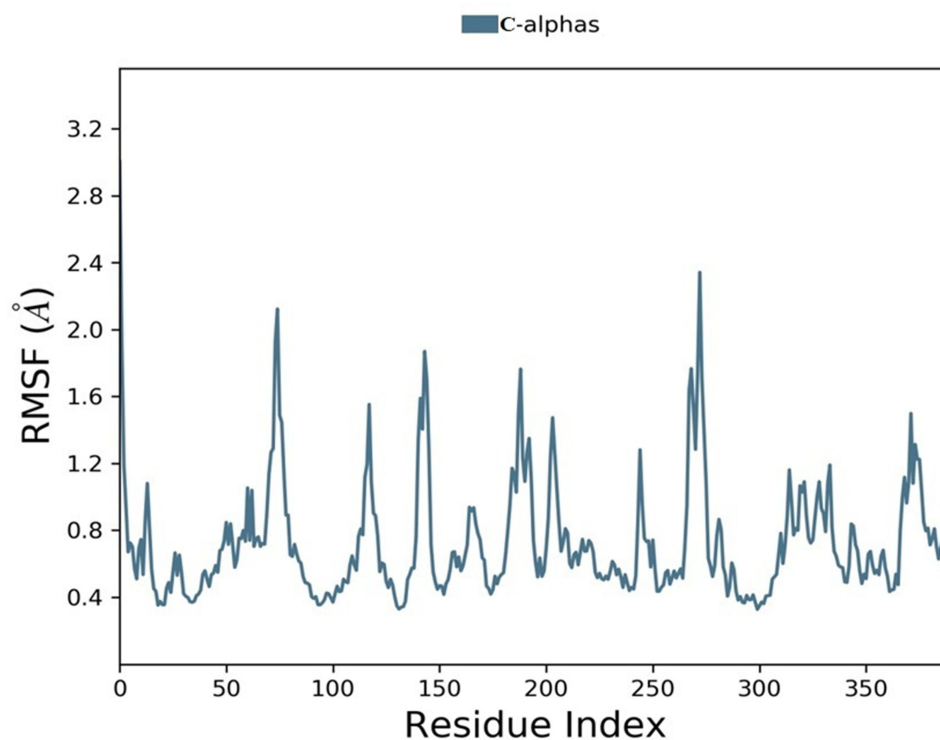
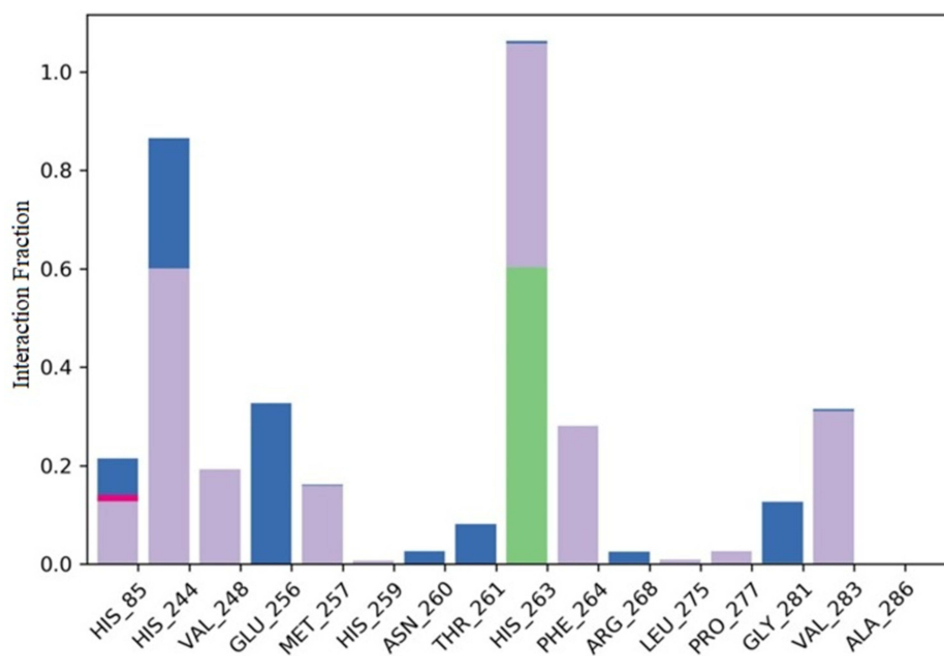


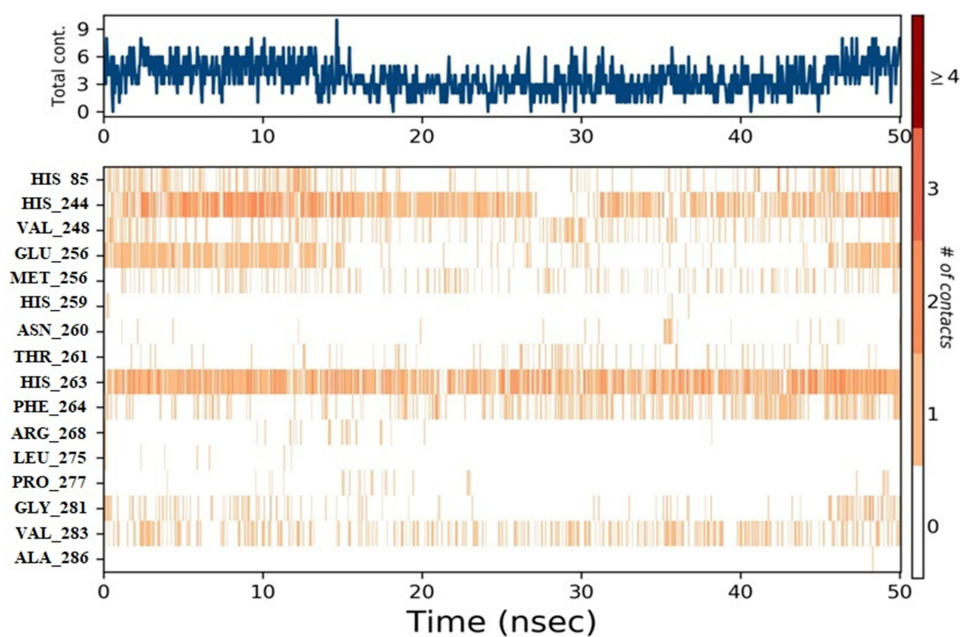
Figure 8 RMSF plot of 2Y9X with Compound 2.

## Conclusion

This study reports the synthesis of anthraquinone-cyclopentanone derivatives (1–8) and the evaluation of their 1,1-diphenyl-2-picryl hydroxyl free radical scavenging, tyrosinase inhibitory, antibacterial and cytotoxic activities. Accordingly, compound



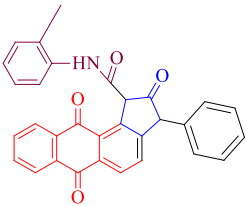
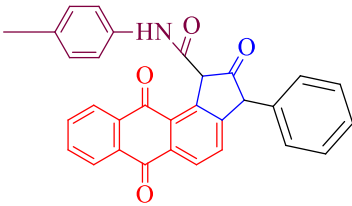
**Figure 9** Histogram of protein-ligand contacts of 2Y9X with compound 2.



**Figure 10** Timeline representation of protein-ligand contacts of 2Y9X with compound 2. #The Number of conducts.

2 showed significant activity due to the presence of a hydroxyl moiety, which influenced the inhibitory effect on tyrosinase. In the DPPH free radical scavenging test, the anthraquinone compounds demonstrated a moderate level of activity. However, most of the anthraquinone analogues compound (1–8) showed weaker activity than butylatedhydroxytoluene. The anthraquinone analogues showed a moderate level of antibacterial activity compared with that of the reference antibiotic. All compounds (1–8) were significantly less active than the other compounds, and the standard doxorubicin ( $LC_{50}:0.74\pm$

**Table 6** Comparison of Highly Active Compounds and the Structure-Activity Relationship

 <p style="text-align: center;">Compound 1</p>		 <p style="text-align: center;">Compound 2</p>	
<b>Tyrosinase Inhibition activities (IC<sub>50</sub> (µg/mL))</b>			
77.62 ± 1.20		13.45 ± 0.24	
<b>Cytotoxic activity</b>			
87.0 ± 0.16		82.34 ± 0.16	
<b>Antioxidant activity (100 µg/mL)</b>			
58.11		39.08	
<b>Antibacterial activity [mm]</b>			
<b>S. aureus</b>	<b>E. coli</b>	<b>S. aureus</b>	<b>E. coli</b>
10	–	10	8

0.01 µg/mL). Compound 2 showed docking scores of (–8.6 kcal/mol) for the 2Y9X protein and (–4.7 kcal/mol) for kojic acid. Compound 2 is better for launching molecular dynamics simulations to validate the molecular docking study and to confirm the stability of the obtained compounds. Compound 2 was developed based on the concept of a “one drug-multiple targets” strategy, which sought to target multiple disease pathways simultaneously to create a novel therapeutic agent. Further research into the mechanisms involved may increase the likelihood of their development as promising skin-whitening agents.

## Acknowledgments

The authors extend their appreciation to the Researchers Supporting Project Number [RSP2024 R393], King Saud University, Riyadh, Saudi Arabia

## Disclosure

The authors declare no conflicts of interest in this work.

## References

- Demir Y. Naphthoquinones, benzoquinones, and anthraquinones: molecular docking, ADME and inhibition studies on human serum paraoxonase-1 associated with cardiovascular diseases. *Drug Dev Res.* 2022;81(5):628–636. doi:10.1002/ddr.21667
- Demir Y, Özslan MS, Duran HE, Küfrevioğlu ÖI, Beydemir Ş. Inhibition effects of quinones on aldose reductase: antidiabetic properties. *Environ Toxicol Pharmacol.* 2019;70:103195. doi:10.1016/j.etap.2019.103195
- Owens J, Voskian S, Murray AT, et al. In-situ production of hydrogen peroxide via electrochemical reduction of anthraquinone electrodes. In 2019 AICHE Annual Meeting; 2019;11:AICHE.
- Demir Y, Ceylan H, Türkeş C, Beydemir Ş. Molecular docking and inhibition studies of vulpinic, carnosic and usnic acids on polyol pathway enzymes. *J Biomol Struct.* 2022;40:12008–12021. doi:10.1080/07391102.2021.1967195
- Jiang D, Wang F, Lan B, et al. Efficient treatment of anthraquinone dye wastewater by adsorption using sunflower torus-like magnesium hydroxide microspheres. *Korean J Chem Eng.* 2020;37:434–447. doi:10.1007/s11814-019-0455-z
- Jin J, Luo Y, Zhou C, et al. Synthesis of indeno[1,2-c]furans via a Pd-catalyzed bicyclization of 2-alkynylidobenzene and propargylic alcohol. *J Org Chem.* 2012;77(24):11368–11371. doi:10.1021/jo302223y
- Prabhakar KR, Veerapur VP, Bansal P, et al. Identification and evaluation of antioxidant, analgesic/anti-inflammatory activity of the most active ninhydrin-phenol adducts synthesized. *Bioorg Med Chem.* 2006;14:7113–7120. doi:10.1016/j.bmc.2006.06.068

8. Türkeş C, Demir Y, Beydemir Ş. In vitro inhibitory activity and molecular docking study of selected natural phenolic compounds as ar and sdh inhibitors. *Chemistry Select.* 2022;7:202204050. doi:10.1002/slct.202204050
9. Liu J, Wu F, Chen C. Design and synthesis of aloë-emodin derivatives as potent anti-tyrosinase, antibacterial and anti-inflammatory agents. *Bioorg Med Chem.* 2015;25(22):5142–5146. doi:10.1016/j.bmcl.2015.10.004
10. Selvaraj K, Daoud A, Alarifi S, Idhayadhulla A. Tel-Cu-NPs catalyst: synthesis of naphtho [2, 3-g] phthalazine derivatives as potential inhibitors of tyrosinase enzymes and their investigation in kinetic, molecular docking, and cytotoxicity studies. *Catalysts.* 2020;10:1442. doi:10.3390/catal10121442
11. Malik MS, Alsantali RI, Jassas RS, et al. Journey of anthraquinones as anticancer agents – a systematic review of recent literature. *RSC Adv.* 2021;11(57):35806–35827. doi:10.1039/D1RA05686G
12. Bhatarraí G, Choi JW, Seong SH, Nam TJ, Jung HA, Choi JSA-I. anti-glycation, anti-tyrosinase and CDK4 inhibitory activities of alaternin (= 7-hydroxyemodin). *Nat Prod Sci.* 2021;27:28–35. doi:10.20307/nps.2021.27.1.28
13. Masi M, Evidente A. Fungal bioactive anthraquinones and analogues. *Toxins.* 2020;12:714. doi:10.3390/toxins12110714
14. Qun T, Zhou T, Hao J, et al. Antibacterial activities of anthraquinones: structure–activity relationships and action mechanisms. *RSC Med Chem.* 2023;14:1446–1471. doi:10.1039/D3MD00116D
15. Stasevych M, Zvorych V, Novikov VS. A computational approach in the search of new biologically active 9, 10-anthraquinone derivatives. *IDDM.* 2020;3:178–185.
16. Li Y, Jiang JG. Health functions and structure–activity relationships of natural anthraquinones from plants. *Food & Function.* 2018;9:6063–6080. doi:10.1039/C8FO01569D
17. Bhasin AK, Chauhan P, Chaudhary S. A novel sulfur-incorporated naphthoquinone as a selective “turn-on” fluorescence chemical sensor for rapid detection of Ba<sup>2+</sup> ion in semi-aqueous medium. *Sensors and Actuators B.* 2019;294:116–122. doi:10.1016/j.snb.2019.04.098
18. Kumar P, Ghosh A, Jose DA. A simple colorimetric sensor for the detection of moisture in organic solvents and building materials: applications in rewritable paper and fingerprint imaging. *Analyst.* 2019;144:594–601. doi:10.1039/C8AN01042K
19. Bayrak S, Öztürk C, Demir Y, Alım Z, Küfrevioğlu ÖI. Purification of polyphenol oxidase from potato and investigation of the inhibitory effects of phenolic acids on enzyme activity. *Protein Pept.* 2020;27:187–192. doi:10.2174/0929866526666191002142301
20. Saini Y, Khajuria R, Rana LK, et al. Unprecedented reaction of ninhydrin with ethyl cyanoacetate and diethyl malonate on ultrasonic irradiation. *Tetrahedron.* 2016;72:257–263. doi:10.1016/j.tet.2015.11.022
21. Ahmed N. Chapter 8 - synthetic advances in the indane natural product scaffolds as drug candidates: a review. *Stud Nat Prod Chem.* 2016;51:383–434.
22. He G, Wu C, Zhou J, et al. A Method for Synthesis of 3-Hydroxy-1-indanones via Cu-Catalyzed Intramolecular Annulation Reactions. *J Org Chem.* 2018;83:13356–13362. doi:10.1021/acs.joc.8b02149
23. Beydemir Ş, Demir Y. Antiepileptic drugs: impacts on human serum paraoxonase-1. *J Biochem Mol Toxicol.* 2017;31:e21889. doi:10.1002/jbt.21889
24. Obaid RJ, Mughal EU, Naeem N, et al. Natural and synthetic flavonoid derivatives as new potential tyrosinase inhibitors: a systematic review. *RSC Adv.* 2021;11:22159–22198. doi:10.1039/D1RA03196A
25. Palabiyık E, Sulumer AN, Uguz H, et al. Assessment of hypolipidemic and anti-inflammatory properties of walnut (*Juglansregia*) seed coat extract and modulates some metabolic enzymes activity in triton WR-1339-induced hyperlipidemia in rat kidney, liver, and heart. *J Mol Recognit.* 2023;36:e3004. doi:10.1002/jmr.3004
26. Özaslan MS, Sağlantaş R, Demir Y, Genç Y, Saraçoğlu İ, Gülçin İ. Isolation of some phenolic compounds from *Plantagosubulata* L. and determination of their antidiabetic, anticholinesterase, antiepileptic and antioxidant activity. *Chem Biodivers.* 2022;19:e202200280. doi:10.1002/cbdv.202200280
27. Lourenço-Lopes C, Fraga-Corral M, Jimenez-Lopez C, et al. Metabolites from macroalgae and its applications in the cosmetic industry: a circular economy approach. *Resources.* 2020;9:101. doi:10.3390/resources9090101
28. Yaşar Ü, Gönül İ, Türkeş C, Demir Y, Beydemir Ş. Transition-metal complexes of bidentate Schiff-base ligands: in vitro and in silico evaluation as non-classical carbonic anhydrase and potential acetylcholinesterase inhibitors. *ChemistrySelect.* 2021;6:7278–7284. doi:10.1002/slct.202102082
29. Spraggon G, Koesema E, Scarselli M, et al. Supramolecular organization of the repetitive backbone unit of the *Streptococcus pneumoniaepilus*. *PLoS One.* 2010;5:10919. doi:10.1371/journal.pone.0010919
30. Jiang L, Ma Y, Chen Y, et al. Multi-target antibacterial mechanism of ruthenium polypyridine complexes with anthraquinone groups against *Staphylococcus aureus*. *RSC Med Chem.* 2023;14:700–709. doi:10.1039/D2MD00430E
31. Alhadrami HA, Abdulaal WH, Hassan HM, Alhakamy NA, Sayed AM. In silico-based discovery of natural anthraquinones with potential against multidrug-resistant *E. coli*. *Pharm.* 2022;15:86. doi:10.3390/ph15010086
32. Vedhagiri K, Manilal A, Valliyammai T, et al. Antimicrobial potential of a marine seaweed *Asparagopsis taxiformis* against *Leptospira javanica* isolates of rodent reservoirs. *Ann Microbiol.* 2009;59:431–437. doi:10.1007/BF03175127
33. Zeng HJ, Sun DQ, Chu SH, Zhang JJ, Hu GZ, Yang R. Inhibitory effects of four anthraquinones on tyrosinase activity: insight from spectroscopic analysis and molecular docking. *Int J Biol Macromol.* 2020;160:153–163. doi:10.1016/j.ijbiomac.2020.05.193
34. Muddathir AM, Yamauchi K, Batubara I, Mohieldin EAM, Mitsunaga T. Anti-tyrosinase, total phenolic content and antioxidant activity of selected Sudanese medicinal plants. *S Afr J Bot.* 2017;109:9–15. doi:10.1016/j.sajb.2016.12.013
35. Cui HX, Duan FF, Jia SS, Cheng FR, Yuan K. Antioxidant and tyrosinase inhibitory activities of seed oils from *torreyagrandis* fort. *Ex Lindl. Biomed Res Int.* 2018;2018. doi:10.1155/2018/5314320
36. Xia L, Idhayadhulla A, Lee YR, Wee YJ, Kim SH. Anti-tyrosinase, antioxidant, and antibacterial activities of novel 5-hydroxy-4-acetyl-2, 3-dihydronaphtho [1, 2-b] furans. *Eur J Med Chem.* 2014;86:605–612. doi:10.1016/j.ejmech.2014.09.025
37. Mostafa AA, SathishKumar C, Al-Askar AA, Sayed SR, SurendraKumar R, Idhayadhulla A. Synthesis of novel benzopyran-connected pyrimidine and pyrazole derivatives via a green method using Cu (II)-tyrosinase enzyme catalyst as potential larvicidal, antifeedant activities. *RSC Adv.* 2019;9:25533–25543. doi:10.1039/C9RA04496E
38. Mullaivendhan J, Ahamed A, Raman G, Radhakrishnan S, Akbar I. Synthesis and antibacterial activity of pyrano [3, 2-g] chromene-4, 6-dione derivatives and their molecular docking and DFT calculation studies. *Results Chem.* 2023;6:101175. doi:10.1016/j.rechem.2023.101175

39. Idhayadhulla A, Manilal A, Ahamed A, Alarifi S, Raman G. Potato Peels Mediated Synthesis of Cu (II)-nanoparticles from Tyrosinase Reacted with bis-(N-aminoethylethanolamine)(Tyr-Cu (II)-AEEA NPs) and Their Cytotoxicity against Michigan Cancer Foundation-7 Breast Cancer Cell Line. *Mol.* 2021;26:6665. doi:10.3390/molecules26216665
40. Mullaivendhan J, Akbar I, Gatasheh MK, et al. Cu (II)-catalyzed: synthesis of imidazole derivatives and evaluating their larvicidal, antimicrobial activities with DFT and molecular docking studies. *BMC Chem.* 2023;17:155. doi:10.1186/s13065-023-01067-1
41. Abuthakir MHS, Sharmila V, Jeyam M. Screening *Balanitesaegyptiaca* for inhibitors against putative drug targets in *Microsporiumgypseum*–Subtractive proteome, docking and simulation approach. *Infect Genet Evol.* 2021;90:104755. doi:10.1016/j.meegid.2021.104755
42. Mani A, Ahamed A, Ali D, et al. Dopamine-mediated vanillin multicomponent derivative synthesis via grindstone method: application of antioxidant, anti-tyrosinase, and cytotoxic activities. *Drug Des DevelTher.* 2021;15:787–802. doi:10.2147/DDDT.S288389
43. Rezaei M, Mohammadi HT, Mahdavi A, Shourian M, Ghafouri H. Evaluation of thiazolidinone derivatives as a new class of mushroom tyrosinase inhibitors. *Int J Biol Macromol.* 2018;108:205–213. doi:10.1016/j.ijbiomac.2017.11.147
44. Adeniji OO, Ojemaye MO, Okoh AI. Antibacterial activity of metallic nanoparticles against multidrug-resistant pathogens isolated from environmental samples: nanoparticles/antibiotic combination therapy and cytotoxicity study. *ACS Appl Bio Mater.* 2022;5:4814–4826.
45. Salah DB, Chakchouk-Mtibaa A, Mellouli L, et al. Novel 3-phenyl-1-(alkylphenyl)-9-oxa-4-azaphenanthren-10-ones as inhibitors of some enzymes: synthesis, characterization, biological evaluation and molecular docking studies. *J Biomol Struct.* 2022;1–17. doi:10.1080/07391102.2022.2114938
46. Halawa AH, Elgammal WE, Hassan SM, et al. Synthesis, anticancer evaluation and molecular docking studies of new heterocycles linked to sulfonamide moiety as novel human topoisomerase types I and II poisons. *Bioorg Chem.* 2020;98:103725.
47. Velmurugan L, Ahamed A, Idhayadhulla A, Alarifi S, Gurusamy R. Antioxidant, antibacterial, and cytotoxic activities of Cimemoxin derivatives and their molecular docking studies. *J King Saud Univ Sci.* 2023;103011. doi:10.1016/j.jksus.2023.103011
48. Qi Y, Liu Y, Zhang B, et al. Comparative antibacterial analysis of the anthraquinone compounds based on the AIM theory, molecular docking, and dynamics simulation analysis. *J Mol Model.* 2023;29:16. doi:10.1007/s00894-022-05406-2
49. Cardoso R, Valente R, Souza da Costa CH, et al. Analysis of kojic acid derivatives as competitive inhibitors of tyrosinase: a molecular modeling approach. *Mole.* 2021;26:2875. doi:10.3390/molecules26102875
50. Feng S, Wang W. Bioactivities and structure–activity relationships of natural tetrahydroanthraquinone compounds: a review. *Front Pharmacol.* 2020;11:799. doi:10.3389/fphar.2020.00799

## Drug Design, Development and Therapy

Dovepress

### Publish your work in this journal

Drug Design, Development and Therapy is an international, peer-reviewed open-access journal that spans the spectrum of drug design and development through to clinical applications. Clinical outcomes, patient safety, and programs for the development and effective, safe, and sustained use of medicines are a feature of the journal, which has also been accepted for indexing on PubMed Central. The manuscript management system is completely online and includes a very quick and fair peer-review system, which is all easy to use. Visit <http://www.dovepress.com/testimonials.php> to read real quotes from published authors.

Submit your manuscript here: <https://www.dovepress.com/drug-design-development-and-therapy-journal>